ELSEVIER

Journal of Alloys and Compounds 434–435 (2007) 472–476

Journal of ALLOYS AND COMPOUNDS

www.elsevier.com/locate/jallcom

The effects of process control agents on mechanical alloying behavior of a Fe–Zr based alloy

R. Juárez, J.J. Suñol *, R. Berlanga, J. Bonastre, L. Escoda

University of Girona, EPS, Campus Montilivi s/n, Girona 17071, Spain

Available online 26 September 2006

Abstract

In this work, a Fe–Zr based alloy prepared by MA was investigated. The as-milled powders were characterized using X-ray diffraction, differential scanning calorimetry, induction coupled plasma, chemical analysis and scanning electron microscopy. Analysis shows small contamination (<1.8 at.%) from the milling tools. In MA process, cold welding between particle and particle, and fracturing of the cold welded particles under high energy collision are involved. The balance between cold welding and fracturing can be controlled by the addition of a surface additive, a process control agent (PCA). Various PCAs such as: methanol, stearic acid, cyclohexane and PBTC were used. The results indicate that the impurities introduced by the PCAs may produce considerable effects on the thermally induced crystallization process as well as on the structural behaviour of the as milled powders, if compared with material synthesized without surfactant. We obtain materials with higher thermal stability and low crystalline size (∼6 nm). Nevertheless, in other samples the formation of a carbide and/or oxide phase or a high crystallite size (>60 nm) was found.

Keywords: B mechanical alloying; Process controlled agents; Fe based materials

1. Introduction

Mechanical alloying (MA) is a solid state process capable to obtain metastable structures like amorphous and nanocrystalline materials [1,2].

During MA, powder particles are subjected to high-energy collisions, which causes the powder particles to be cold-welded together and fractured [3]. A process control agent (PCA) is a surface additive normally used in the milling processes in order to control the balance between the fracture and welding. The mechanism lies in the modification of the surface condition of the deformed particles by impeding the clean powder to powder contact necessary for cold welding [4]. The type of PCA also plays an important role in the balance. Several PCAs, such as cyclohexane [5], hexane [6], stearic acid [7], methanol [8], ethyl acetate [9] or polyethylene glycol [10], are often used in MA.

In this work we have investigated the effect and the role of different PCAs on the structural, compositional and thermal evolution of the alloy structure of a FeNiZrB alloy produced by MA.

2. Materials and methods

Elemental Fe and B with a Ni_7Zr_3 compound powdered particles were milled in a Fritsch P7 planetary ball mill operated at 600 rpm. The composition of the alloy is $Fe_{70}(Ni_7Zr_3)_{15}B_{15}$. To avoid the influence of oxidation during milling, the vial was filled with Ar gas before milling. In order to investigate the effects of the species of PCA on the MA mechanism, methanol (CH_3OH), PBTC ($C_7H_{11}O_9P$), cyclohexane (C_6H_{12}) and stearic acid ($CH_3(CH_2)_{16}CO_2H$) were chosen. As much as 3 ml of PCA were added to the powders. The ball to powder weight ratio was 5:1.

Morphology evolution was followed by means of scanning electron spectroscopy (SEM) using a Zeiss DSM960 equipment. In order to evaluate contamination from milling tools and PCAs, elemental and chemical analysis were performed by energy dispersive X-ray spectroscopy (EDX) using a Si–Li detector and Tracor EDX analyzer, by induction coupled plasma spectroscopy (ICP) in a Liberty-RL ICP Varian equipment and by chemical analysis in a CE Instruments 1110.

Thermal analysis was performed under Ar atmosphere (flow rate: 40 ml min^{-1}). Isochronal crystallization kinetics was studied in a DSC30 Mettler–Toledo differential scanning calorimeter. X-ray diffraction (XRD) patterns were carried out in a D-500 Siemens equipment using Cu K_α radiation

3. Results and discussion

The morphology of the powders was analyzed by scanning electron microscopy. Fig. 1 shows three micrographs which correspond to samples milled for 80 h of the alloys with cyclohexane (B) and methanol (C) as PCA, and the alloy without PCA (A).

* Corresponding author. Tel.: +34 972 419757; fax: +34 972 418098.
E-mail address: joanjosep.sunyol@udg.es (J.J. Suñol).

0925-8388/$ – see front matter © 2006 Elsevier B.V. All rights reserved.
doi:10.1016/j.jallcom.2006.08.108

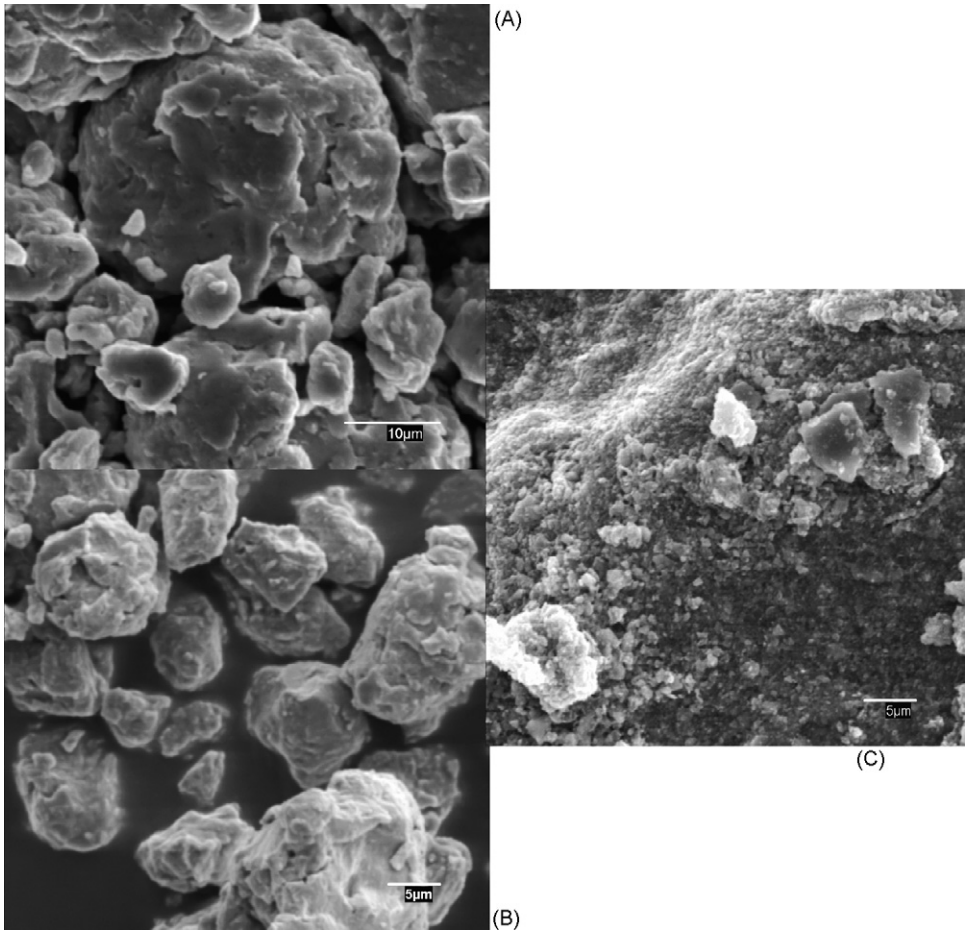

Fig. 1. SEM micrographs of samples milled for 80 h. (A) Sample without PCA, (B) with cyclohexane and (B) with methanol (C).

The as-milled powder has a relatively broad distribution of particle size. Usually, the average particle size diminishes with the increase of the milling time [11] as shown in Table 1. Lower value, at about 12 μm, corresponds to alloy milled with cyclohexane. The topology of methanol sample indicates a higher specific surface if compared with ductile shapes of the other micrographs.

In MA processes, a serious problem is the potential for significant contamination from the milling media (balls and vial) or atmosphere as well as the formation of non desired phases like oxides, hydrides, nitrides or carbides [12,13]. Furthermore, the milling of fine powders with organic PCAs containing atoms such as O, C, H, etc., may affect the process. For MA samples, the contamination is favoured by the high surface/volume ratio of the small particles. The contamination measured by EDX and ICP in the powdered alloy increases with the milling time. Nevertheless, the results show only slight (<1.8 at.%) contamination from the solid milling tools (Fe, Ni and Cr) after 40–80 h MA. The values are similar in all alloys. Furthermore, several microanalysis were performed and the carbon and oxygen presence was detected as shown in Table 2. As expected, the lower contamination values correspond to the non-PCA alloy. The cyclohexane and stearic acid samples present small contamination if compared with PBTC and methanol samples.

Fig. 2 shows the X-ray diffraction patterns obtained for the alloys milled for 80 h. The majority of the X-ray diffraction peaks correspond to the bcc Fe phase. Furthermore, carbide (Fe_3C) is found in PBTC and methanol samples, and magnetite (Fe_3O_4), only in the methanol sample. Thus, methanol and PBTC are not the most indicated PCA, at least in the milling conditions chosen. Furthermore, the sample with stearic acid has larger nanocrystalline size, about 68 nm, as determined by Williamson–Hall analysis. Only the alloy milled with cyclohexane has broader peaks, probably due to the formation of a more disordered phase, that sample milled without PCA.

Table 1
Average particle size of the samples milled for 40 and 80 h

MA time (h)	Without PCA	Methanol	PBTC	Cyclohexane	Stearic acid
40	18	40	30	15	19
80	15	30	25	12	16

Table 2
C and O contamination in samples milled for 80 h

Element	Without PCA	Methanol	PBTC	Cyclohexane	Stearic acid
C	0.01	11.8	2.7	1.2	3.1
O	1.4	19.2	9.4	1.4	2.9

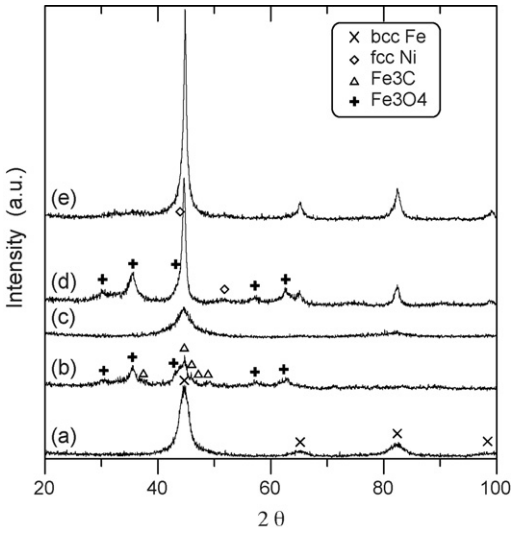

Fig. 2. XRD patterns of samples milled for 80 h: (a) without PCA, (b) methanol, (c) cyclohexane, (d) PBTC and (e) stearic acid.

Fig. 3 shows the differential scanning calorimetry curves of the mechanically alloyed powders. There is a broad hump in the temperature range of 100–300 °C. The humps are associated with the relief of internal stresses, since no phase transformations were detected in X-ray diffraction and Mössbauer studies performed in alloys with similar composition [14,15]. The exothermic peaks over 300 °C correspond to the crystallization processes. Cyclohexane and non-PCA samples have similar thermal crystallization behaviour: two peaks, one at low temperature (near 400 °C) and a main process. This main process is about 40 °C displaced to higher temperature in the case of cyclohexane. Other alloys present a temperature broad process.

The apparent activation energy, E, for the crystallization processes of alloys milled 80 h was obtained in order to investigate how the PCA affects the crystallization behaviour. It was evaluated using the Kissinger equation relating $\ln(\beta/T_p^2)$ and

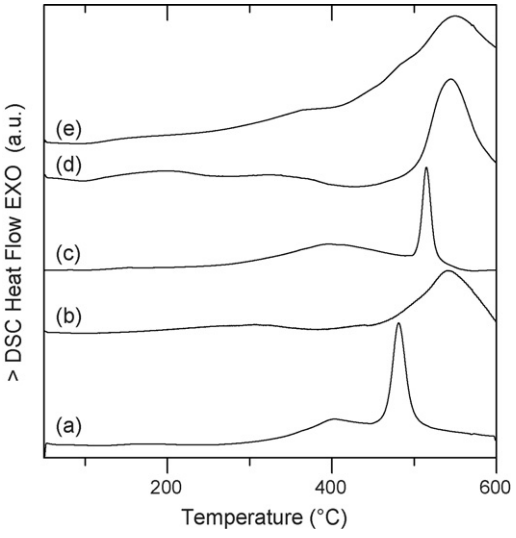

Fig. 3. DSC scans at 10 K min^{-1} of samples milled for 80 h: (a) without PCA, (b) methanol, (c) cyclohexane, (d) PBTC and (e) stearic acid.

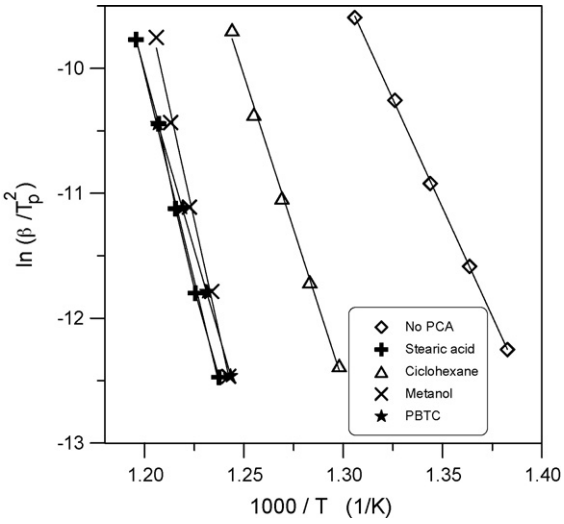

Fig. 4. Kissinger plots of the main crystallization process of alloys milled for 80 h.

$1/T_p$ with β the heating rate and T_p the peak temperature [16]. The crystallization data have been collected from DSC thermograms, obtained with different heating rates (2.5, 5, 10, 20 and 40 K min^{-1}). Fig. 4 shows the Kissinger plot with the linear fittings corresponding to the main crystallization process. The values range between 599 and 288 kJ mol^{-1}. The lower value corresponds to the alloy without PCA and the higher to the methanol sample, the condition containing most O atoms. This tendency is similar to that reported for the Ni–50 at.% Zr [17] and Ti–Al [18] systems. In the Ni–Zr system the activation energy for crystallization increased from 240 to 290 kJ mol^{-1} by addition of 2.3 at.% O. The values of the minor first crystallization process, between 155 and 193 kJ mol^{-1} seem reasonably to be associated with a grain growth process [19]. A high defect of the lattice, the immense magnification of the boundary surface and high diffusion rate lead to low activation energies for the

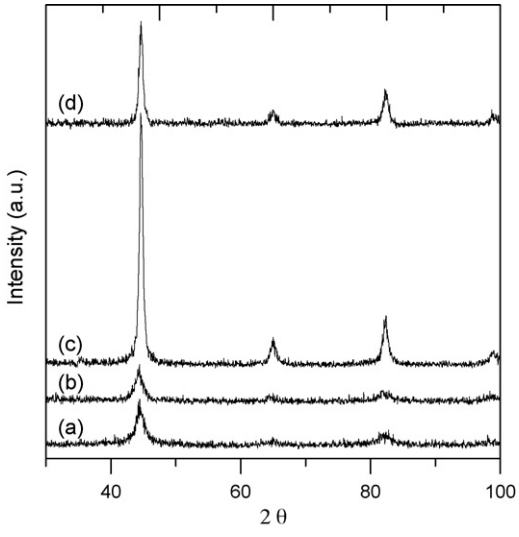

Fig. 5. XRD patterns of samples milled for 80 h after annealing during 30 min: (a) at 400 °C without PCA, (b) at 400 °C with methanol, (c) at 500 °C without PCA and (d) at 500 °C with stearic acid.

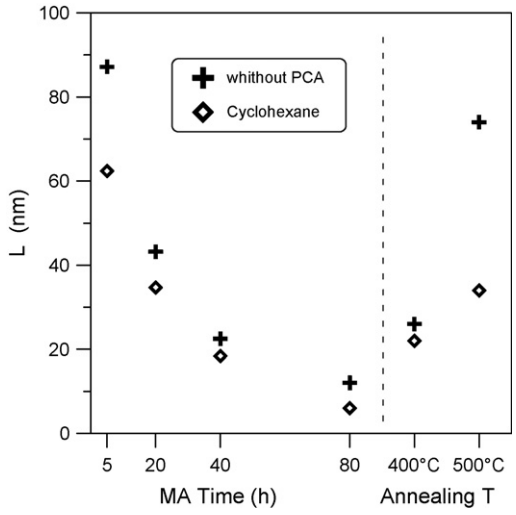

Fig. 6. Crystalline size, L, as a function of milling time and annealing treatment obtained from Williamson–Hall analysis.

transformation of the structure [20]. Similar results were found in other Fe(Zr, Nb, Ni) based alloys [21,22].

The combination of higher activation energy and crystallization temperature indicates high thermal stability of the structure obtained after milling. From previous results, it is clear that the best candidate to be compared to the sample without PCA is the cyclohexane sample. Fig. 5 shows the crystallization products of cyclohexane and non-PCA samples after annealing treatment during 30 min at 400 and 500 °C, corresponding to the peak position of the first crystallization process and to the end of the main crystallization process of the sample without PCA respectively. In all cases, the XRD patterns show a nanocrystalline state. Figs. 6 and 7 show the crystallite size, L, and the lattice strain, ε, as a function of milling time and annealing temperature obtained using the Williamson–Hall method [23]. The parameters obtained are shown in Figs. 6 and 7. As expected, the increase of the milling time favors the reduction of the nanocrystalline size to values of 6 nm (cyclohexane) and 11 nm (without PCA) and an increase of the lattice strain. Ulterior thermal treatments induce the growth of the nanocrystalls size. After annealing at 400 °C, the values are of 22–26 nm. The results after annealing at 500 °C confirm the higher thermal stability of the nanocrystalline phase in the sample with cyclohexane as PCA. It is known that the carbon from the decomposition of an organic PCA as hexane increases the formation of a disordered phase in the Fe–B system by C dissolution in the disordered phase without the formation of crystalline carbide [24].

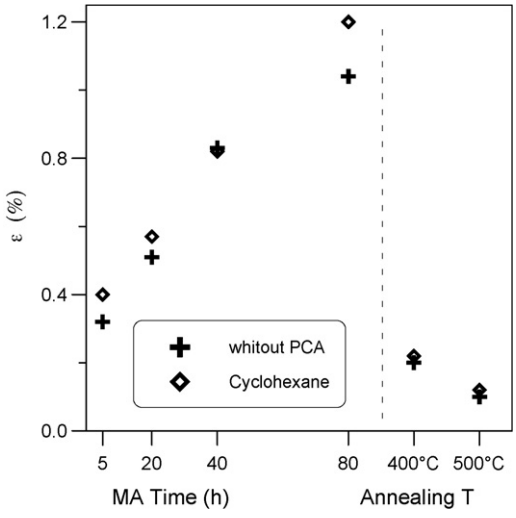

Fig. 7. Lattice strain, ε, as a function of milling time and annealing treatment obtained from Williamson–Hall analysis.

4. Conclusions

The $Fe_{70}(Ni_7Zr_3)_{15}B_{15}$ alloy was obtained by MA of powders using methanol, PBTC, cyclohexane and stearic acid as process control agents. The XRD analysis shows the formation of a nanocrystalline phase (crystallite size: 6–68 nm). The increase of the milling time favours the reduction of the nanocrystalline size and an increase of the lattice strain. Furthermore, the carbide (Fe_3C) phase is found in PBTC and methanol samples, and magnetite (Fe_3O_4) in the methanol sample. Moreover, the sample with stearic acid has the larger nanocrystalline size.

Structural relaxation at low temperature and two crystallization processes were found from DSC scans. Using Kissinger analysis, the lowest apparent activation energy of the main crystallization process corresponds to the alloy without PCA and the highest to the O rich methanol sample. The values of the minor first crystallization process, between 155 and 193 kJ mol^{-1} seem reasonably to be associated with a grain growth process.

Ulterior thermal treatments induce the growth of the nanocrystalls. Annealing analysis confirm the higher thermal stability of the nanocrystalline phase in the sample with cyclohexane as PCA, probably due to C dissolution.

Acknowledgements

Financial support from MICYT (project No. MAT2003-08271-C02) and DURSI (project 2001SGR-00190) is acknowledged. J.B. also agrees a MCYT fellowship.

References

[1] M.E. McHenry, M.A. Willard, D.E. Laughlin, Prog. Mater. Sci. 44 (1999) 291.
[2] J.J. Suñol, Mater. Sci. Forum 269 (1998) 175–180.
[3] J.S. Benjamin, Mater. Sci. Forum 88–90 (1992) 1.
[4] L. Liu, Y.F. Zhang, J. Alloys Compd. 290 (1999) 279–283.
[5] P. Bhattacharya, P. Bellon, R.S. Averback, S.J. Hales, J. Alloys Compd. 368 (2004) 187–196.
[6] R.B. Schwarz, P.B. Desch, S.R. Srinlvasan, Proceedings of the Second International Conference on Estructural Applications of Mechanical Alloying, ASM International, Vancouver, 1993, p. 15.
[7] J.S. Byun, J.H. Shim, Y.W. Cho, J. Alloys Compd. 365 (2004) 149–156.
[8] A. Palacios-Lazcano, J.G. Cabanas-Moreno, F. Gandarilla-Cruz, Scripta Mater. 52 (2005) 571–575.
[9] X.P. Xiu, PhD Thesis at KULeuven, Belgium (1991) 34.
[10] Y.F. Zhang, L. Lu, S.M. Yap, J. Mater. Process. Technol. 89-90 (1999) 260–265.
[11] L. Lu, Y.F. Zhang, J. Alloys Compd. 290 (1999) 279–283.
[12] K.Y. Wang, T.D. Shen, M.X. Quan, J.T. Wang, Scripta Metall. 26 (1992) 9336.

[13] Z. Caamaño, G. Pérez, L.E. Zamora, S. Suriñach, J.S. Muñoz, M.D. Baró, J. Non-Cryst. Sol. 287 (2001) 15–19.
[14] J.J. Suñol, T. Pradell, N. Clavaguera, M.T. Clavaguera-Mora, Mater. Sci. Forum 360–363 (2001) 525–530.
[15] J.J. Suñol, A. González, J. Saurina, L.L. Escoda, T. Pradell, M.T. Clavaguera-Mora, N. Clavaguera, Mater. Sci. Eng. A 375 (2004) 881–887.
[16] H. Kissinger, Anal. Chem. 29 (1957) 1702.
[17] G. Cocco, I. Soletta, L. Battezatti, M. Barocco, S. Enzo, Philos. Mag. B 61 (1990) 473–486.
[18] W. Lee, S.I. Kwun, J. Alloys Compd. 240 (1996) 193–199.
[19] J.J. Suñol, A. González, J. Saurina, J. Thermal Anal. Calorim. 72 (2003) 329–335.
[20] A.H. Mansour, J. Barry, J. Mater. Sci. Lett. 17 (1998) 1127.
[21] P. Duhaj, I. Matko, P. Svec, J. Sitek, D. Janickovic, Mater. Sci. Eng. B 39 (1996) 208–213.
[22] J.J. Suñol, T. Pradell, N. Clavaguera, M.T. Clavaguera-Mora, Philos. Mag. 83 (2003) 2323–2342.
[23] A. Revesz, T. Ungar, A. Borbely, J. Lendvai, Nanostruct. Mater. 7 (1996) 779–788.
[24] P. Ruuskanen, O. Heczko, J. Non-Cryst. Sol. 224 (1998) 36–42.